

1
2
3
4
5
6
7
8
9
10
11
12
13
14
15
16

Bone union-promoting effect of romosozumab
in a rat posterolateral lumbar fusion model
(ラット腰椎後側方固定術(PLF)モデルにおける
Romosozumab 投与による骨癒合促進効果に関する検討)

千葉大学大学院医学薬学府
先端医学薬学専攻
(主任：大鳥 精司教授)
金 勤東

17 **Abstract**

18 This study investigated the effect of romosozumab on bone union in a rat posterolateral lumbar
19 fixation model. Posterolateral lumbar fixation was performed on 8-week-old male Sprague
20 Dawley rats (n=20). For bone grafting, autogenous bone (40 mg) was harvested from the spinous
21 processes of the 10th thoracic vertebra until the 2nd lumbar vertebra and implanted between the
22 intervertebral joints and transverse processes of the 4th and 5th lumbar vertebrae on both sides.
23 Rats were matched by body weight and equally divided into two groups: R group (Evenity®, 25
24 mg/kg) and control (C) group (saline). Subcutaneous injections were administered twice a week
25 until 8 weeks after surgery. Computed tomography was performed at surgery and week 8 after
26 surgery. The area and percentage of bone trabeculae in the total area of bone fusion were
27 calculated. Statistical analysis was performed using an unpaired *t*-test ($P<0.05$). We found that
28 the R group rats had significantly higher mean bone union rate and volume than did the C group
29 rats at all time courses starting week 4 after surgery. The R group had significantly higher
30 increase rates than did the C group at weeks 4 and 6 after surgery. The percentage of bone
31 trabeculae area in the R group was approximately 1.7 times larger than that in the C group. Thus,
32 we demonstrated that romosozumab administration has stimulatory effects on bony outgrowth at
33 bone graft sites. We attribute this to the modeling effect of romosozumab.

34 **1. INTRODUCTION**

35 Because the proportion of aged people is increasing in the population, in recent years there has
36 been an increase in the rate of spinal fusion surgery performed for osteoporotic patients.

37 However, serious postoperative complications have often been observed, including postoperative
38 vertebral fracture and pedicle screw (PS) loosening. According to a study on cadavers,

39 osteoporotic patients tend to have a weak pull-out strength and PS loosening (1). As the number
40 of spinal surgeries for patients with severe osteoporosis is expected to increase further, there is an
41 urgency to prevent postoperative complications and achieve favorable postoperative outcomes.

42 A variety of osteoporosis drugs (e.g., bisphosphonate, and a preparation of human parathyroid
43 hormone) have been used thus far to effect bone remodeling and improve bone strength. The
44 bone remodeling process consists of three stages: bone resorption stage, where bone resorption
45 by osteoclasts is initiated; transitional stage, the intermediary stage between bone resorption and
46 bone formation; and bone formation stage, where new bone is formed (2). This process is also
47 consistent with bone union after spine surgery. Of interest is that various osteoporosis drugs have
48 been recently reported to also promote bone union (3,4).

49 In particular, romosozumab, which has been recently introduced in Japan, is receiving increasing
50 attention in this regard. Romosozumab is a human immunoglobulin monoclonal antibody that
51 binds to sclerostin (a bone formation suppressor) to inhibit its action. Sclerostin is an
52 extracellular inhibitor of the canonical Wnt signaling pathway and is secreted by osteocytes. As
53 romosozumab specifically binds to sclerostin and prevents it from binding to lipoprotein
54 receptor-related protein 5 (LRP5) and lipoprotein receptor-related protein 6 (LRP6), it thus
55 inhibits the suppression of the canonical Wnt signaling in osteoblast lineage cells (5-7).

56 Activation of the canonical Wnt pathway increases mass and strength of cortical and spongy

57 bone by promoting bone formation and inhibiting bone resorption. The pre-marketing clinical
58 trial data have also demonstrated increased bone formation and decreased bone resorption. Thus,
59 within one month of romosozumab administration, the bone resorption marker C-terminal
60 telopeptide (CTX) in the blood decreased by approximately 35% (statistically significant) and a
61 mean for the bone formation marker P1NP of approximately 95% (statistically significant) were
62 reported (6).

63 Therefore, we propose that romosozumab exhibits a bone union effect. However, only a few
64 studies on its therapeutic effects in clinical practice have been conducted because it has only
65 recently been introduced in Japan. Therefore, this study aimed to conduct basic research to
66 investigate the bone union-promoting effect of romosozumab in a rat spinal fusion model.

67

68 **2. METHODS**

69 **2.1 Experimental animals**

70 The study protocol was conducted in accordance with the National Institutes of Health
71 Guidelines for the Care and Use of Laboratory Animals (2011 revision) and approved by the
72 Ethics Committee of Chiba University (8). We used 8-week-old Sprague Dawley male rats
73 (n = 20; 200-250 g, Japan SLC Inc., Shizuoka, Japan).

74 **2.2 Posterolateral lumbar fusion (PLF) surgery**

75 All rats were injected intraperitoneally with a mixture of three anesthetic agents, namely Domitor
76 0.15 ml/kg (Nippon Zenyaku Kogyo Co., Ltd., Japan), Dormicum 2 mg/kg (Astellas Pharma Inc.,
77 Japan), and Vetorphale 2.5 mg/kg (Meiji Seika, Ltd., Japan), or saline 1.45 ml/kg (Otsuka
78 Pharma Inc., Japan). Subsequently, an antimicrobial agent (Ampicillin Sodium 20,000 U/kg,

79 Meiji Seika, Japan) was administered subcutaneously before surgery (9).
80 The vertebral arch and transverse process of the 4th/5th lumbar vertebrae on the left and right
81 sides, and the 4th/5th lumbar intervertebral joint were exposed after performing a skin incision
82 along the dorsal part of the median line and separating the fascia from the paraspinal muscle on
83 both sides. We harvested 40 mg of graft bone from the spinous process of the 10th thoracic
84 vertebra to the 2nd lumbar vertebra. We placed the graft bones between the intervertebral joint
85 and the transverse process of the 4th/5th lumbar vertebrae on the left and right sides as
86 autogenous bone graft (Figure 1) (8, 10, 11). The fascia and skin were sutured using 4-0
87 absorbable thread. Postoperatively, all rats were kept in cages where they could eat and drink
88 freely (9).

89 **2.3 Experimental groups**

90 To avoid body size differences, we divided the rats sequentially into two equal groups based on
91 body weight: the romosozumab group (herein, R group) and the control group (herein, C group).
92 Rats in the R group were injected subcutaneously with romosozumab (Evenity[®], sclerostin
93 antibody 105 mg/1.17 mL, calcium acetate hydrate 2.41 mg/1.17 mL [13 mM], acetic anhydride
94 2.04 mg/1.17 mL [17 mM], sucrose 70 mg/1.17 mL (6%), polysorbate-20 0.070 mg/1.17 mL
95 [0.006%] at pH 5.2, ©Amgen Inc., Thousand Oaks, CA), at a dose of 25 mg/kg twice a week
96 (Tuesday and Friday mornings) for 8 weeks (Table 1). Animals in the C group were injected with
97 an equivalent volume of saline (Otsuka Pharma Inc., Japan) (11,12).

98 **2.4 Evaluation tests**

99 **2.4.2 Micro-computed tomography examination**

100 Micro-computed tomography (CT) examination was performed under isoflurane inhalation

101 (1.5% isoflurane [Mylan, Canonsburg, PA,]) to evaluate the volume of bone union area (13). The
102 bone graft site was scanned using a CT apparatus (in vivo micro-CT system, R_mCT2, Rigaku
103 Co., Tokyo, Japan) before surgery and every two weeks until week 8 (resolution of 59 μm , tube
104 voltage of 90 kV, tube current of 200 μA , field of view 30 mm, and an exposure time of 26 s)
105 (Table 1) (9). Three spinal surgeons unrelated to the study evaluated the sagittal, coronal, and
106 axial image data on the rate of bone union between the intervertebral joint and the transverse
107 process in both groups, and the mean value was used (14). The reliability of the bone union rate
108 results was then assessed by intraclass correlation coefficients (ICC) with intra-examiner error. A
109 comparative review of the volume of bone union area using Ziostation2 (Ziosoft Inc., Tokyo,
110 Japan) was conducted as a quantitative evaluation for bone union (Figure 2) (15).

111 **2.4.3 Bone densitometry**

112 Rats were euthanized by anesthetic overdose on week 8. The right femur from the right hip joint
113 was collected and scanned using the CT apparatus mentioned earlier. The bone mineral density
114 (BMD) (expressed as mgHA/cm^3) of each rat was measured from the obtained image using
115 dedicated software (Bone analysis software, Rigaku Co., Ltd. Austin, TX) (12, 16, 17).

116 **2.4.4 Histological examination**

117 We collected the lumbar vertebrae after euthanasia (9). After paraffin block was prepared using
118 10% neutral buffer formalin (0.1 M, pH 7.4) by fixation, 2- μm -thick transverse sections were
119 made and stained with hematoxylin and eosin (8).
120 The transected images of PLF region were generated using a fluorescence microscope (BZ-X800,
121 Keyence Corp., Osaka, Japan). The total area of the PLF region was calculated using a dedicated
122 microscopic measurement software (Hybrid Cell Count Module BZ-H4C Analyzer software,

123 Keyence Corp., Osaka, Japan). Six images (20-fold magnification) were randomly selected from
124 PLF transverse images, and the area percentage of trabecular bone for each image was calculated
125 and compared (Figure 3) (18).

126 **2.5 Statistical Analyses**

127 Data comparisons for each group were statistically analyzed using an unpaired *t*-test, and
128 statistical significance was set at $P < 0.05$.

129

130 **3. RESULTS**

131 **3.1 CT examination**

132 Primary CT images for each group are shown in Figure 4a-f. There was no significant difference
133 in the mean bone union rate between the intervertebral joint and transverse process in the two
134 groups at week 2 after surgery; however, the mean bone union rate in the R group was
135 significantly higher than that in the C group at all time points after week 4 (Group R vs. Group
136 C: 47.0±3.3% vs. 37.0±2.8%, week 4; 79.0±3.1% vs. 61.0±3.6%, week 6; and 97.5±2.5% vs.
137 84.0±3.6%, week 8) (all $P < 0.05$) (Figure 5). The ICCs with intra-examiner error were
138 ICC(1,3)=0.996 and ICC(2,3)=0.931; there was no disagreement among examiners.

139 There was also no significant difference in the volume of bone union area between the period
140 immediately after surgery and at week 2 after surgery in the two groups; however, the volume of
141 bone union area in the R group was significantly higher than that in the C group at all time points
142 after week 4 (R group vs. C group: 401.83±8.36 mm³ vs. 361.36±13.29 mm³, week 4;
143 483.11±11.81 mm³ vs. 437.25±24.80 mm³, week 6; and 547.46±14.10 mm³ vs. 515.23±11.24
144 mm³, week 8) (all $P < 0.05$) (Figure 6).

145 We also divided the volume at each time point by the volume at the period immediately after
146 surgery, defined as the increase rate. We found that the rate of increase in the R group was
147 significantly greater than that in the C group at weeks 4 and 6 after surgery (R group vs. C group:
148 $1.71 \pm 0.06x$ vs. $1.54 \pm 0.03x$, week 4; $2.06 \pm 0.07x$ vs. $1.86 \pm 0.06x$, week 6) (all $P < 0.05$) (Figure 7).
149 Conversely, there was no significant difference in the rate of increase between the two groups at
150 week 8 after surgery (Figure 7).

151 **3.2 Bone densitometry**

152 The mean BMD of the distal femoral metaphysis was significantly larger in the R group than in
153 the C group (R group vs. C group: 821.1 ± 9.6 mgHA/cm³ vs. 731.1 ± 7.9 mgHA/cm³) ($P <$
154 0.05).

155 **3.3 Histological examination**

156 The pathological images for the left vertebral arch of the 4th lumbar vertebra at week 8 after
157 surgery in the two groups are shown in Figure 8a-d. At week 8 after surgery, there was no
158 significant difference in the mean total PLF area between the two groups (R group: 3.7 ± 0.7 mm²
159 vs. C group: 4.4 ± 0.8 mm²). However, the percentage of bone trabeculae area was significantly
160 larger by approximately 1.7 times in the R group ($61.7 \pm 3.3\%$) than in the C group ($37.2 \pm 1.5\%$)
161 ($P < 0.05$) (Figure 9).

162 **4. DISCUSSION**

163 **4.1 Bone union rate**

164 We found that the mean bone union rate at week 8 after surgery was 82.5% in the C group.
165 Similarly, Kamoda et al. (19) reported a bone union rate of 70% in the same model as assessed

166 using X-ray at week 8 after surgery. The bone union rate was significantly higher in the R group
167 than in the C group at week 4 after surgery, and bone union was noted in almost all rats (97.5%)
168 at week 8 after surgery. Therefore, favorable bone union was clearly achieved from an early
169 stage following romosozumab administration, which can be attributed to the early effect of
170 romosozumab. In a FRAME study for pre-marketing data (6), a statistically significant mean
171 improvement rate in bone resorption marker (CTX) of approximately 35% and a statistically
172 significant mean increase rate in bone formation marker (P1NP) of approximately 95% were
173 reported within a month after administration. Osteoporosis patients also experienced an
174 immediate effect of improvement of abnormal bone metabolism and a high increase in bone
175 density from the early stage after administration (20-22). Thus, we assume that early and reliable
176 bone union was also achieved in this study.

177 **4.2 Volume of bone union area**

178 Although we noted no significant difference in the mean volume of bone union area between the
179 two groups before surgery, it became significantly higher in the R group at week 8. Similar
180 results have been previously reported, although a different model (i.e., rat femur fracture model)
181 was used. For example, Ominski et al. (23) reported that the fracture volume in the R group was
182 significantly higher (41%) than that in the C group as shown by micro-CT scans at week 7 after
183 surgery. McDonald et al. (24) found that the bone regeneration in the R group was significantly
184 higher (26-38%) than that in the C Group as indicated by micro-CT analysis at week 8 after
185 surgery. Thus, romosozumab administration possibly has a stimulatory effect on bony outgrowth
186 at the bone graft site.

187 We attribute this result to the modeling effect of romosozumab. As romosozumab specifically
188 binds to sclerostin and prevents sclerostin from binding to LRP5 and LRP6, it thus inhibits the

189 canonical Wnt signaling in osteoblast lineage cells. The activation of the Wnt signaling pathway
190 leads to increased bone formation and decreased bone resorption, thereby increasing the bone
191 mass of the cortical and trabecular bone (modeling) (6-7). We propose that a similar modeling
192 mechanism occurred in the bone graft site, thereby increasing mean bone union volume
193 following romosozumab administration.

194 **4.3 Bone density**

195 There was a significant increase in bone density of the distal femoral metaphysis following
196 romosozumab administration, indicating that romosozumab increased bone density.

197 **4.4 Pathological findings**

198 We observed that the total PLF area was not significantly different between the two groups, but
199 the percentage of osteophytes for PLF was significantly higher in the R group than in the C
200 group. We also attribute this effect to the previously mentioned modeling effect of romosozumab.
201 Clinical data on osteoporotic patients have revealed that Evenity increases bone density. When
202 we checked the bone volume and microscopic structure during the 12th month as assessed by
203 micro-CT examination of the FRAME study, the volume rate of the trabecular bone was
204 significantly increased following Evenity administration (25). Thus, bone formation due to the
205 active remodeling effect was observed not only in osteoporotic patients, but also in the bone graft
206 site of spinal fusion surgery in this study.

207 ***Limitations of the Study***

208 This study had some limitations. First, the dose of Evenity used in this study was much higher,
209 by approximately 19-fold, than that used in clinical practice (26). Specifically, the adult dose of
210 "210 mg/month" is 3 mg/kg of body weight equivalent to 70 kg, which may be considered an

211 approximately eight times higher dose, and "50 mg/kg subcutaneous injection once/week" in rats
212 is around 19 times higher than the human equivalent (26). If the duration of administration is not
213 taken into account, the exposure dose in this study would be the same as in a previous study (12).
214 Therefore, we plan to conduct additional experiments in the future to examine whether different
215 results would be obtained depending on the dose. Second, the effect of Evenity on BMD was
216 only evaluated in the last observation. Thus, comparing with "before administration" is difficult,
217 and sacrifice is required in our bone-density measuring equipment (because only the size of the
218 femur can be measured). Additionally, most fusions that occur need to undergo a remodeling
219 process to produce the highest functional quality bone in-vivo. We were unable to examine the
220 bone metabolism markers in this study, so it is unclear whether this unionized bone will be
221 remodeled in the future or not. Therefore, additional experiments should be conducted to
222 examine before-and-after effects using a bone metabolism marker (Tracp 5b, etc.). Third, we did
223 not examine bone strength (e.g., three-point bending test) in this study. This may be a limitation
224 of the mechanical testing device (as the model used in this study is only for one intervertebral
225 disc site due to the amount of grafted bone, we cannot conduct further studies using the
226 mechanical testing device because of insufficient length); however, we plan to increase the
227 number of intervertebral disc sites to examine bone strength using bone graft or artificial bone.
228 Fourth, the rat model for posterior spinal fusion has been previously criticized due to its
229 relatively high fusion occurrence rates compared with those in humans, in which it has been
230 reported to have 40% or more non-union rates in non-instrumented fusion surgery (27).
231 Therefore, we believe that the rat model used may be a limitation in this study. Additionally,
232 romosozumab showed a modest improvement in fusion rates beyond 4 weeks (82.5% vs 97%).
233 An important clinical question is how many of the rats would have had true "non-union" of the

234 fusion attempt that was avoided by this drug. If all of the rats eventually evolve a fusion, it would
235 be difficult to assess clinical improvement. In human clinical practice, instrumentation is mostly
236 used for spinal fusion, the bone fusion rate of PLF has been reported as approximately 74% 2-3
237 years after surgery, and there is no discernible difference in clinical outcomes between the union
238 and non-union groups (14, 28, 29). For this reason, we believe that studies using rat models with
239 instrumentation, or animal models described in the literature that document a clinical nonunion
240 mimicking the human condition, should be considered in future research. Fifth, this rat model
241 was not an osteoporotic model; therefore, the results may differ from those using the
242 ovariectomy model. Since the PLF model established in our laboratory was based on this male
243 rat model, we verified the results using the established model first. We plan to use this model for
244 spinal fusion in non-osteoporotic patients. Of note, for the purpose of bone union, this drug is for
245 off-label use; it promotes bone union as a secondary effect of administration in patients with
246 osteoporosis. Therefore, we will consider using the ovariectomy model in the future. Sixth, in
247 Figure 4d, it appears that the fusion is actually across the L3-4 interspace rather than at the L4-5
248 level. It is obvious that localization imaging is not performed in these small animal surgeries. In
249 the surgeries in this study, we always exposed the superior margin of the sacroiliac joint from
250 both iliac crests to confirm the L4-5 level. However, in three of 20 cases, the graft bone was also
251 at the L3-4 level on immediate postoperative CT images. Because L3, L4, and L5 are functional
252 lower lumbar vertebrae, we did not consider the difference in level in this study and determined
253 that it was also one vertebra at the L4-5 level.

254 ***Conclusion***

255 This study examined the effect of romosozumab administration on bone union in a rat lumbar
256 PLF model. We showed that romosozumab administration clearly improved bone union from an

257 early stage and significantly increased the volume of bone union. Thus, these results suggest that
258 romosozumab administration promotes bone union.

259

260 **Acknowledgments**

261 This investigation was supported in part by Grant-in-Aid for Scientific Research of Dr. Sumihisa
262 Orita, Dr. Yawara Eguchi, Dr. Kazuhide Inage and Dr. Yasuhiro Shiga. And we would like to
263 acknowledge all participants for their help in the study.

264 We declare that the research was conducted in the absence of any commercial or financial
265 relationships that could be construed as a potential conflict of interest.

266 **References**

- 267 1. Halvorson TL, Kelley LA, Thomas KA, et al. 1994. Effects of bone mineral density on pedicle
268 screw fixation. *Spine (Phila Pa 1976)*. 19: 2415–2420.
- 269 2. Matsuo K, Irie N. 2008. Osteoclast–osteoblast communication. *Arch Biochem Biophys*. 473:
270 201–209.
- 271 3. Amanat N, McDonald M, Godfrey G, et al. 2007. Optimal timing of a single dose of
272 zoledronic acid to increase strength in rat fracture repair. *J Bone Miner Res*. 22: 867–876.
- 273 4. Ohtori S, Inoue G, Orita S, et al. 2012. Teriparatide accelerates lumbar posterolateral fusion in
274 women with postmenopausal osteoporosis: prospective study. *Spine (Phila Pa 1976)*. 37:
275 1464–1468.
- 276 5. Kendler DL, Bone HG, Massari F, et al. 2019. Bone mineral density gains with a second
277 12-month course of romosozumab therapy following placebo or denosumab. *Osteoporos Int*. 30:
278 2437–2448.
- 279 6. Cosman F, Crittenden DB, Adachi JD, et al. 2016. Romosozumab treatment in postmenopausal
280 women with osteoporosis. *N Engl J Med*. 375: 1532–1543.
- 281 7. Langdahl BL, Libanati C, Crittenden DB, et al. 2017. Romosozumab (sclerostin monoclonal
282 antibody) versus teriparatide in postmenopausal women with osteoporosis transitioning from oral
283 bisphosphonate therapy: a randomised, open-label, phase 3 trial. *Lancet* 390: 1585–1594.
- 284 8. Shiga Y, Orita S, Kubota G, et al. 2016. Freeze-dried platelet-rich plasma accelerates bone
285 union with adequate rigidity in posterolateral lumbar fusion surgery model in rats. *Sci Rep*. 11:
286 36715.
- 287 9. Kaito T, Morimoto T, Kanayama S, et al. 2016 Modeling and remodeling effects of
288 intermittent administration of teriparatide (parathyroid hormone 1-34) on bone morphogenetic

289 protein-induced bone in a rat spinal fusion model. *Bone Rep.* 5: 173–180.

290 10. Hayashi T, Lord EL, Suzuki A, et al. 2016. A comparison of commercially available
291 demineralized bone matrices with and without human mesenchymal stem cells in a rodent spinal
292 fusion model. *J Neurosurg Spine.* 25: 133–137.

293 11. Ominsky MS, Brown DL, Van G, et al. 2015. Differential temporal effects of sclerostin
294 antibody and parathyroid hormone on cancellous and cortical bone and quantitative differences
295 in effects on the osteoblast lineage in young intact rats. *Bone* 81: 380–391.

296 12. Li X, Ominsky MS, Villasenor KS, et al. 2018. Sclerostin antibody reverses bone loss by
297 increasing bone formation and decreasing bone resorption in a rat model of male osteoporosis.
298 *Endocrinology* 159: 260–271.

299 13. Yamamoto T, Hasuike A, Koshi R, et al. 2018. Influences of mechanical barrier permeability
300 on guided bone augmentation in the rat calvarium. *J Oral Sci.* 60: 453–459.

301 14. Kubota G, Kamoda H, Orita S, et al. 2019. Platelet-rich plasma enhances bone union in
302 posterolateral lumbar fusion: A prospective randomized controlled trial. *Spine (Phila Pa 1976).*
303 19: 34–40.

304 15. Hayashi T, Saitoh S, Fukuzawa F, et al. 2017. Noninvasive assessment of advanced fibrosis
305 based on hepatic volume in patients with nonalcoholic fatty liver disease. *Gut Liver.* 11:
306 674–683.

307 16. Suen PK, Zhu TY, Chow DH, et al. 2015. Sclerostin antibody treatment increases bone
308 formation, bone mass, and bone strength of intact bones in adult male rats. *Sci Rep.* 5: 1–9.

309 17. Nakajima S, Inoue T, Huang M, et al. 2020. Does the addition of abiraterone to castration
310 affect the reduction in bone mineral density? *In Vivo* 34: 3291–3299.

311 18. Le Duc D, Lin CC, Popkova Y, et al. 2021. Reduced lipolysis in lipoma phenocopies lipid

312 accumulation in obesity. *Int J Obes (Lond)*. 45: 565–576.

313 19. Kamoda H, Ohtori S, Ishikawa T, et al. 2013. The effect of platelet-rich plasma on
314 posterolateral lumbar fusion in a rat model. *J Bone Joint Surg Am*. 95: 1109–1116.

315 20. Videbaek TS, Christensen FB, Soegaard R, et al. 2006. Circumferential fusion improves
316 outcome in comparison with instrumented posterolateral fusion: long-term results of a
317 randomized clinical trial. *Spine (Phila Pa 1976)*. 31: 2875–2880.

318 21. Lehman RA Jr, Dmitriev AE, Cardoso MJ, et al. Effect of teriparatide [rhPTH(1,34)] and
319 calcitonin on intertransverse process fusion in a rabbit model. *Spine (Phila Pa 1976)*. 35:
320 146–152.

321 22. O’Loughlin PF, Cunningham ME, Bukata SV, et al. 2009. Parathyroid hormone (1-34)
322 augments spinal fusion, fusion mass volume, and fusion mass quality in a rabbit spinal fusion
323 model. *Spine (Phila Pa 1976)*. 34: 121–130.

324 23. Ominsky MS, Li C, Li X, et al. 2011. Inhibition of sclerostin by monoclonal antibody
325 enhances bone healing and improves bone density and strength of nonfractured bones. *J Bone
326 Miner Res*. 26: 1012–1021.

327 24. McDonald MM, Morse A, Birke O, et al. 2018. Sclerostin antibody enhances bone formation
328 in a rat model of distraction osteogenesis. *J Orthop Res*. 36: 1106–1113.

329 25. Chavassieux P, Chapurlat R, Portero-Muzy N, et al. 2019. Bone-forming and antiresorptive
330 effects of Romosozumab in postmenopausal women with osteoporosis: bone histomorphometry
331 and microcomputed tomography analysis after 2 and 12 months of treatment. *J Bone Miner Res*.
332 34: 1597–1608.

333 26. Chouinard L, Felx M, Mellal N, et al. 2016. Carcinogenicity risk assessment of
334 Romosozumab: a review of scientific weight-of-evidence and findings in a rat lifetime

335 pharmacology study. *Regul Toxicol Pharmacol.* 81: 212–222.

336 27. Boden SD, Martin Jr GJ, Morone MA, et al. 1999. Posterolateral lumbar intertransverse
337 process spine arthrodesis with recombinant human bone morphogenetic protein
338 2/hydroxyapatite-tricalcium phosphate after laminectomy in the nonhuman primate. *Spine (Phila*
339 *Pa 1976).* 15: 1179–1185.

340 28. Tsutsumimoto T, Shimogata M, Yoshimura Y, et al. 2008. Union versus nonunion after
341 posterolateral lumbar fusion: a comparison of long-term surgical outcomes in patients with
342 degenerative lumbar spondylolisthesis. *Eur Spine J.* 17:1107–1112.

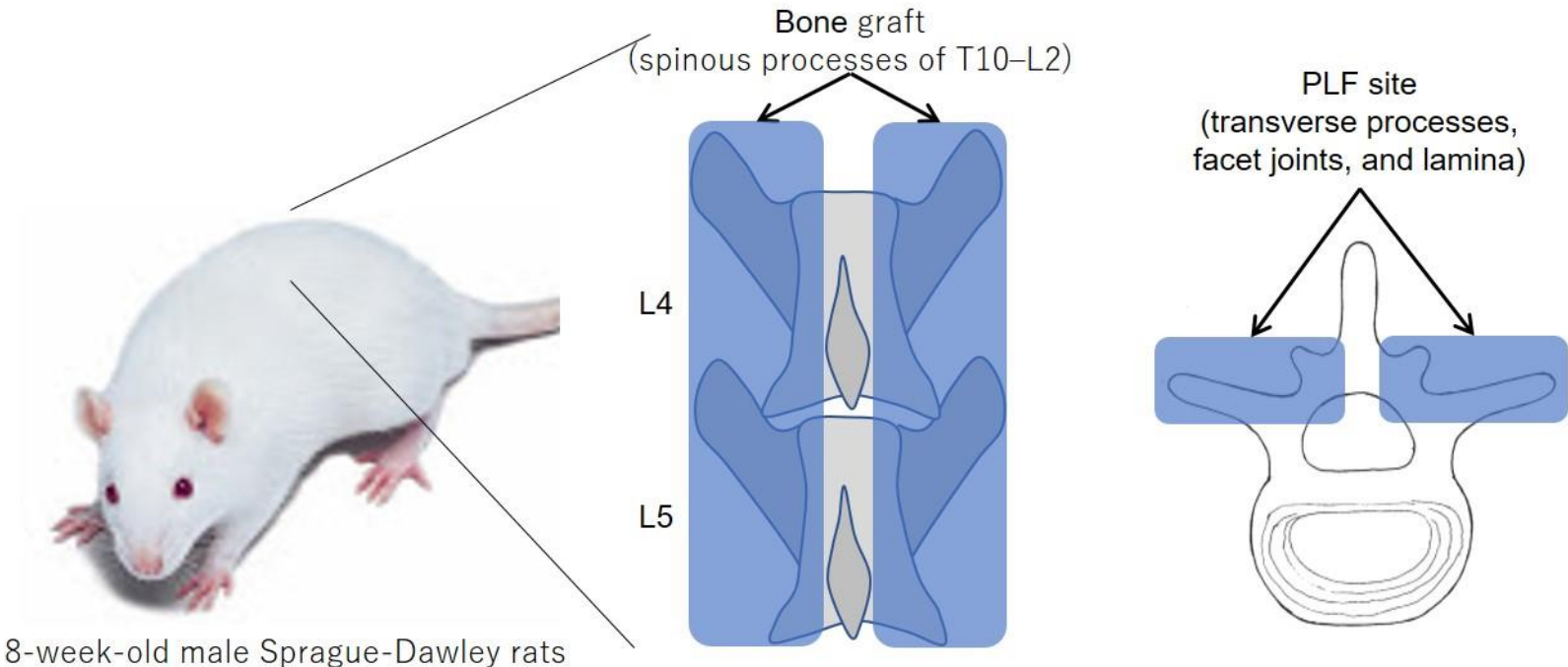
343 29. Ohtori S, Suzuki M, Koshi T, et al. 2011. Single-level instrumented posterolateral fusion of
344 the lumbar spine with a local bone graft versus an iliac crest bone graft: a prospective,
345 randomized study with a 2-year follow-up. *Eur Spine J.* 20:635–639.

346

347

348 **Figure Legends**

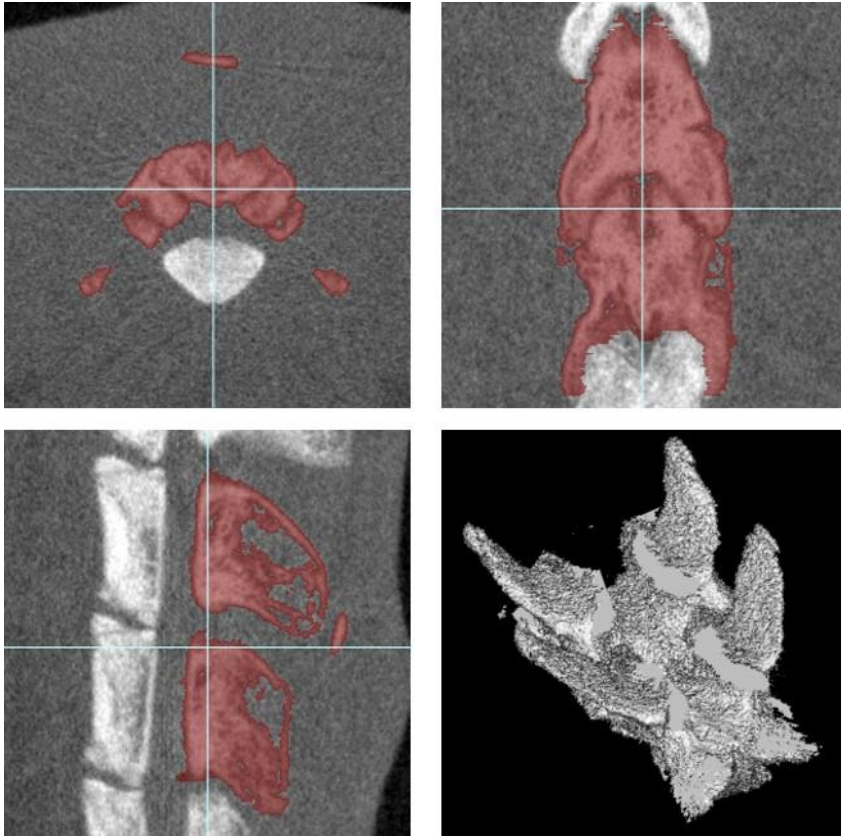
349 Figure 1. The 4th/5th posterolateral lumbar fusion (PLF) surgery.



350

351

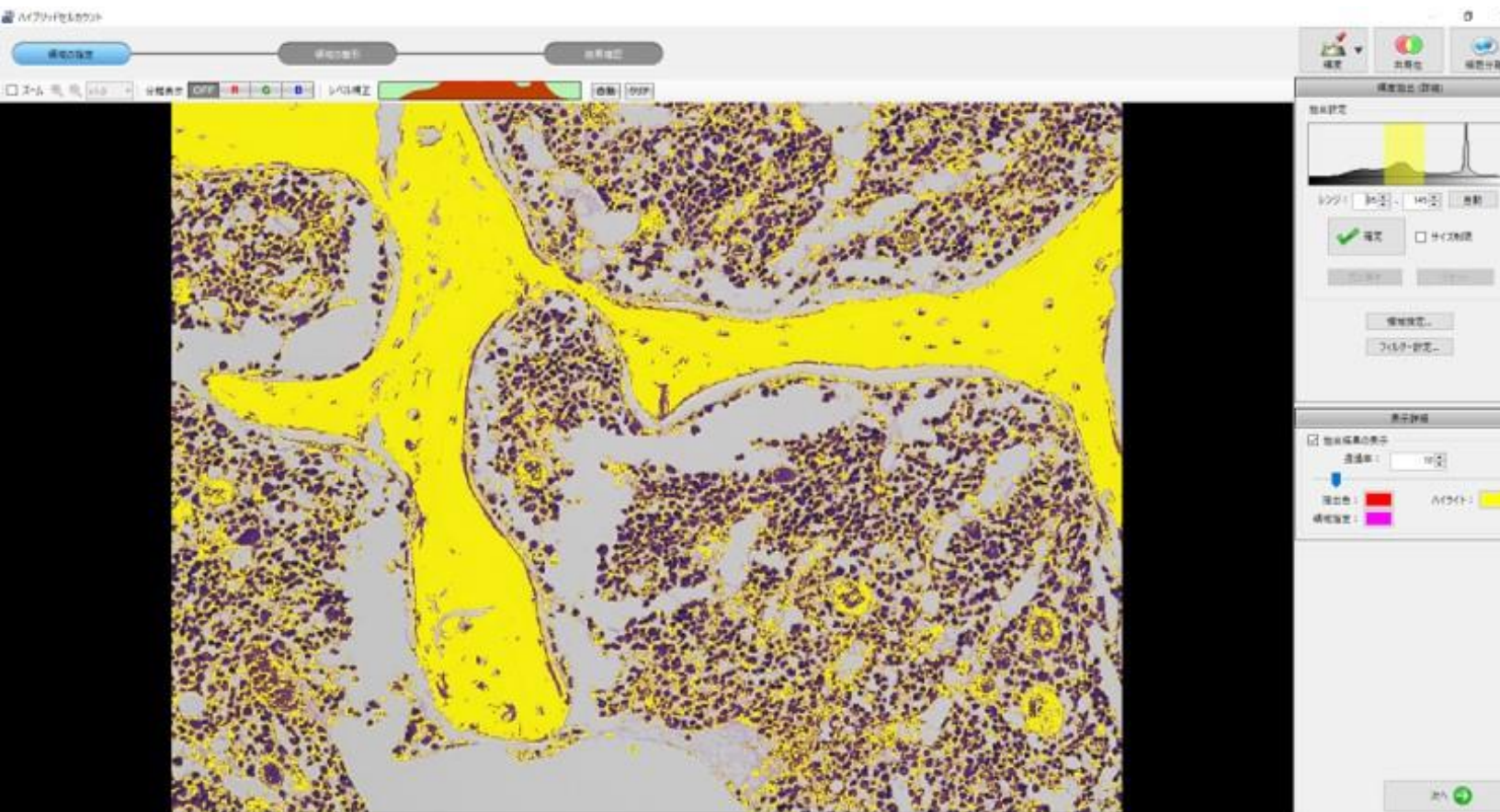
352 Figure 2. Measurement of the volume of the bone union area using Ziostation2 software.



353

354

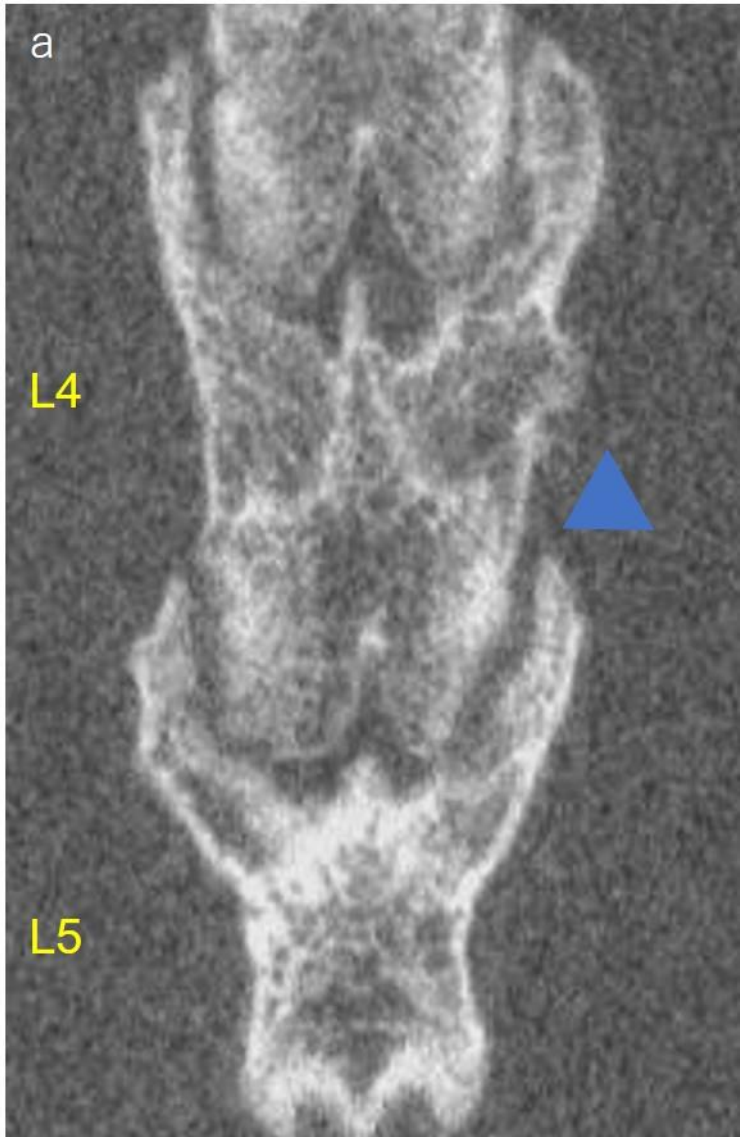
355 Figure 3. Calculation of the area of a trabecular bone using the hybrid cell count module of the
356 BZ-H4C Analyzer software.



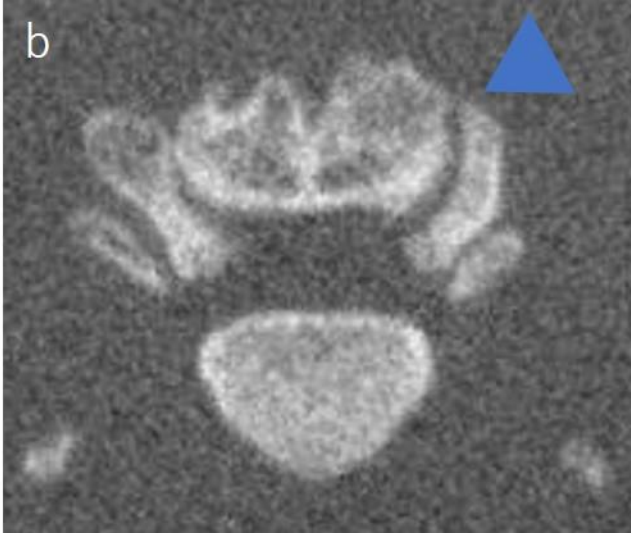
357

358

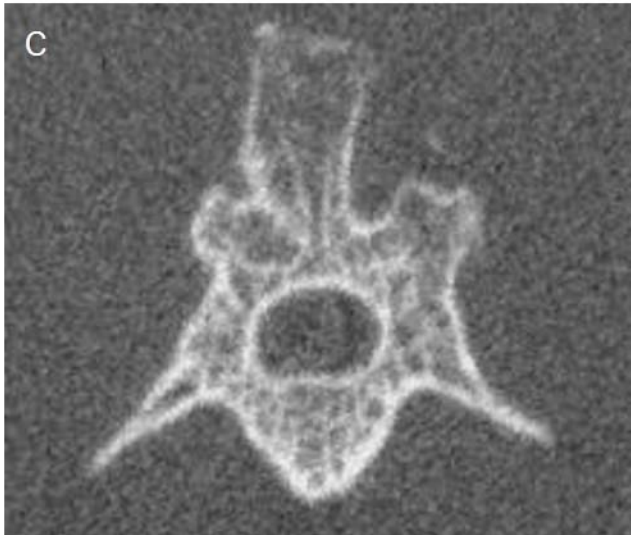
359 Figure 4. Representative CT sections at week 8 post-surgery. a. Coronal section, C group. b.
360 Axial section of the 4th/5th lumbar intervertebral joint, C group. c. Axial section of the 4th
361 lumbar vertebral arch, C group. d. Coronal section of bone union, R group. e. Axial section of the
362 4th/5th lumbar intervertebral joint, R group. f. Axial section of the 4th lumbar vertebral arch, R
363 group.



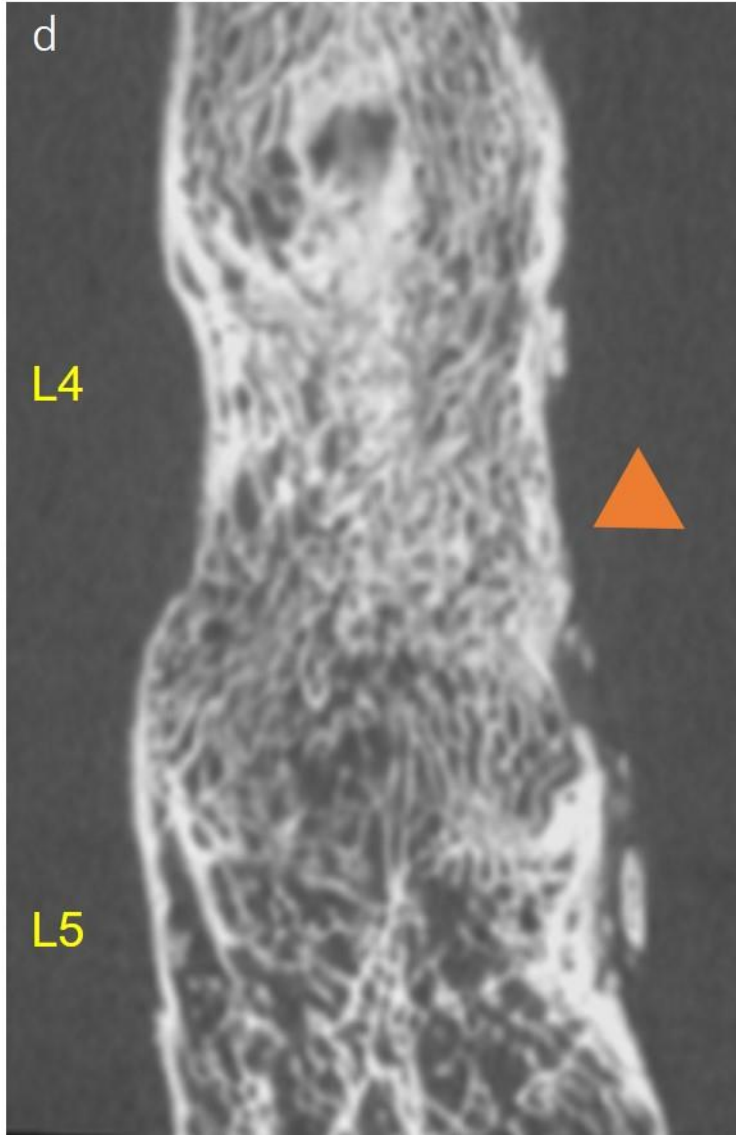
364



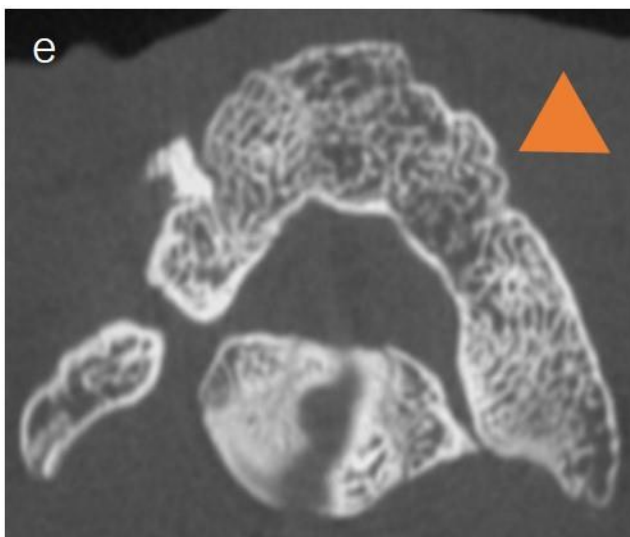
365



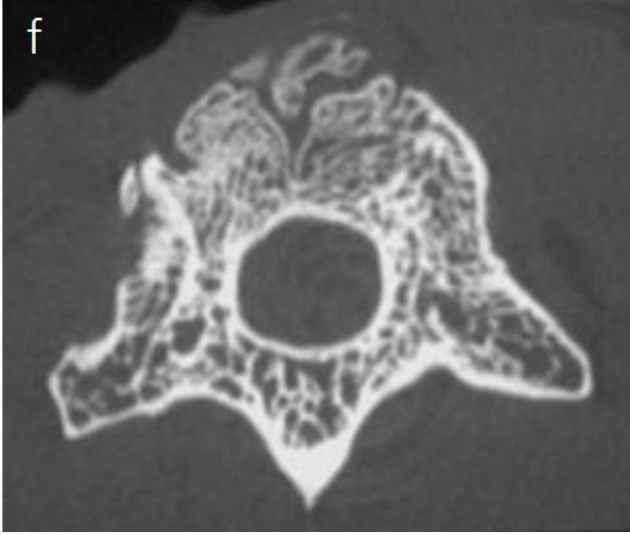
366



367



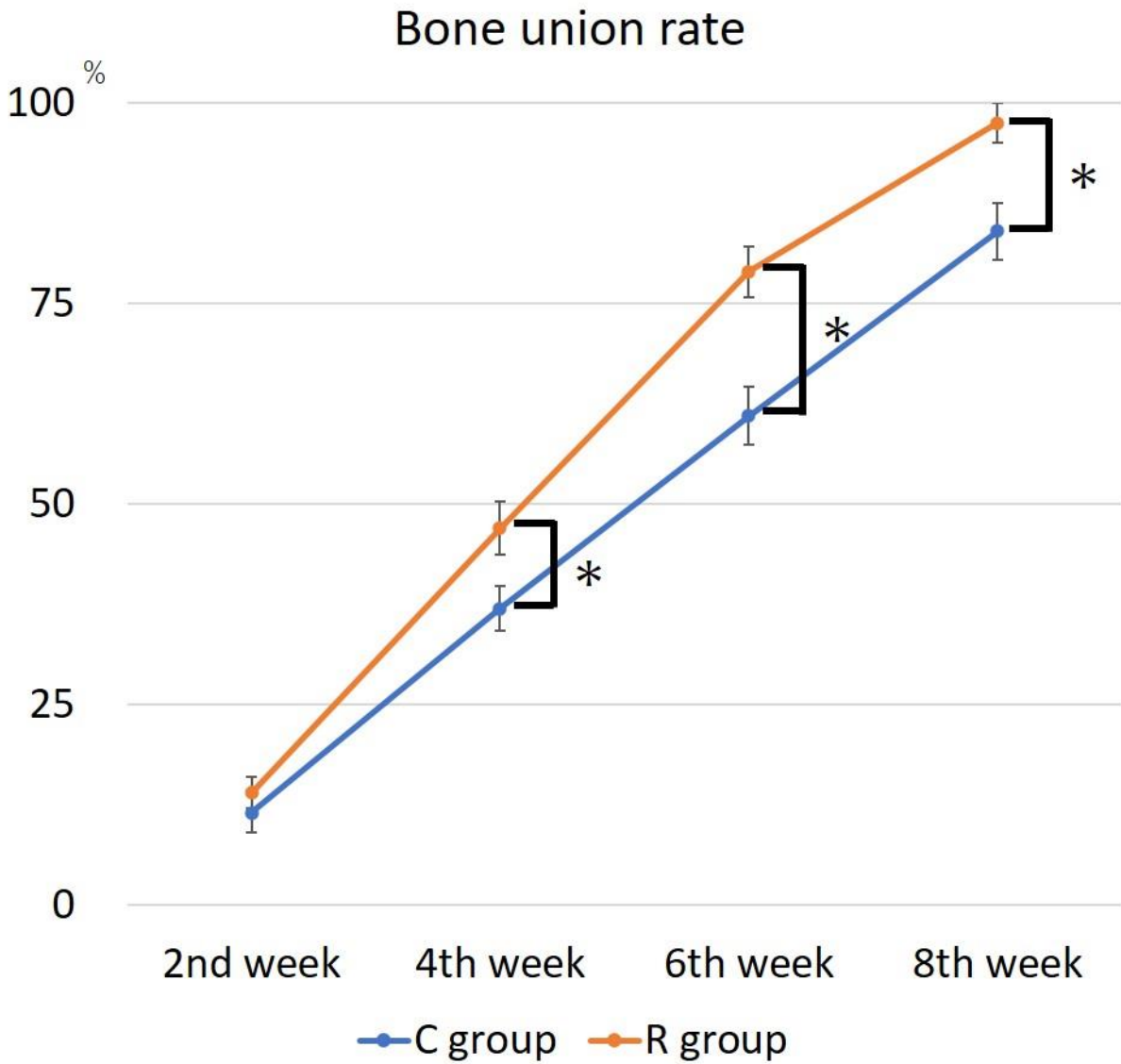
368



369

370

371 Figure 5. Bone union rate between the intervertebral joint and transverse process in the two
372 groups after surgery.



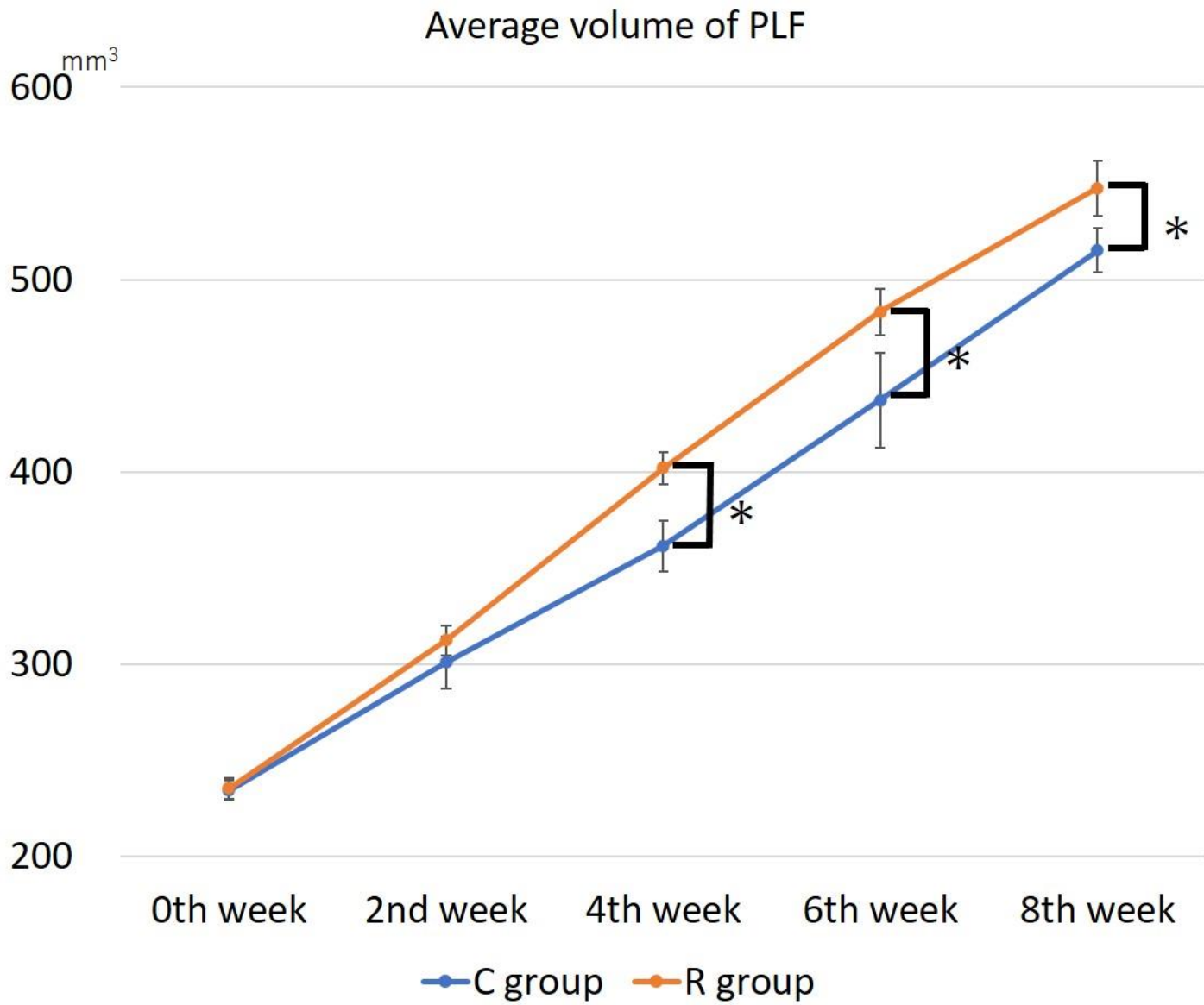
* : p < 0.05 by independent t test

373

374

375

376 Figure 6. Volume of bone union area after surgery.

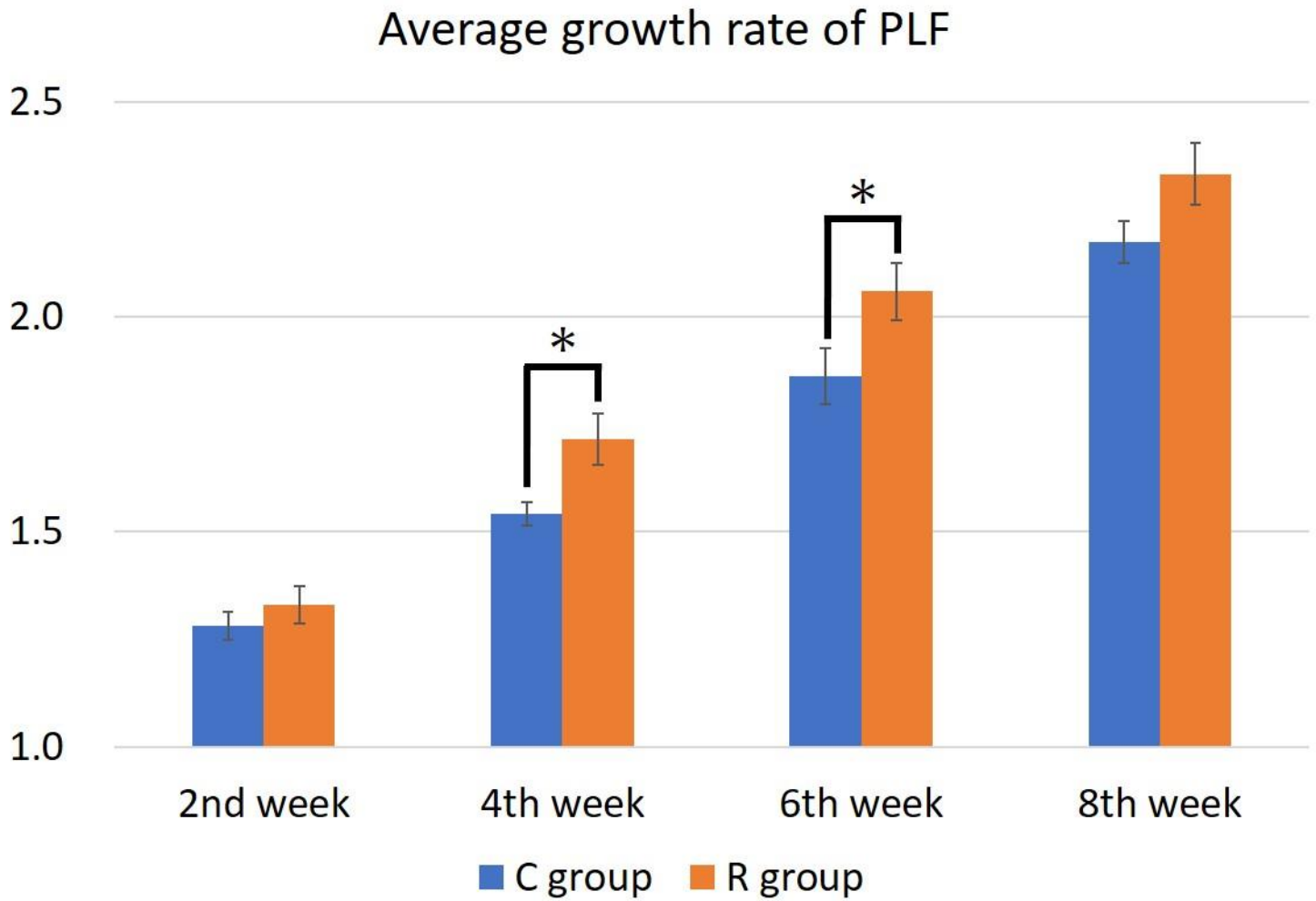


* : p < 0.05 by independent t test

377

378

379 Figure 7. Rate of bone union area increase after surgery.

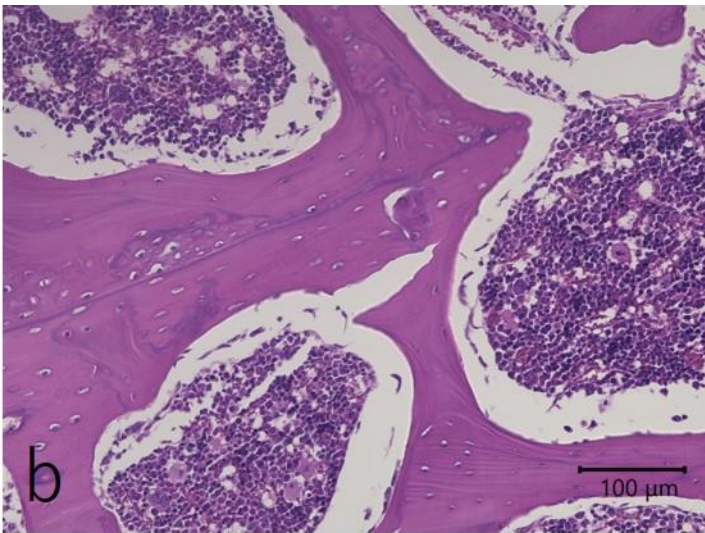
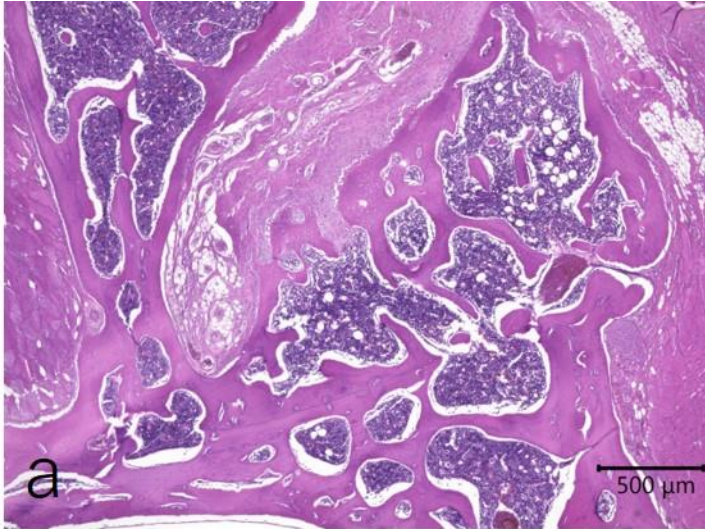


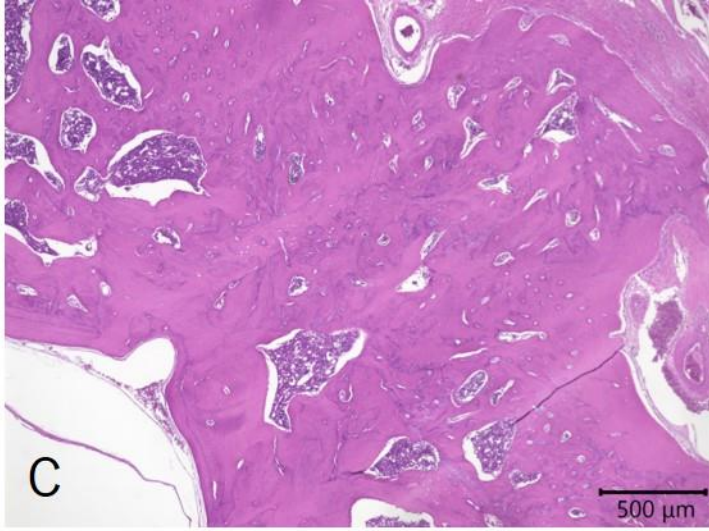
* : p < 0.05 by independent t test

380

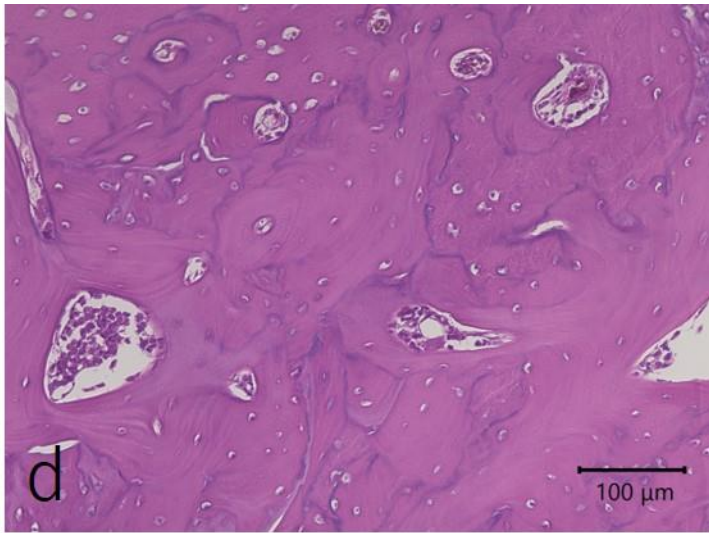
381

382 Figure 8. Pathological images. a-b. Left vertebral arch of the 4th lumbar vertebra, C group. c-d.
383 Left vertebral arch of the 4th lumbar vertebra, R group. a, c: 4× magnification; b, d: 20×
384 magnification.





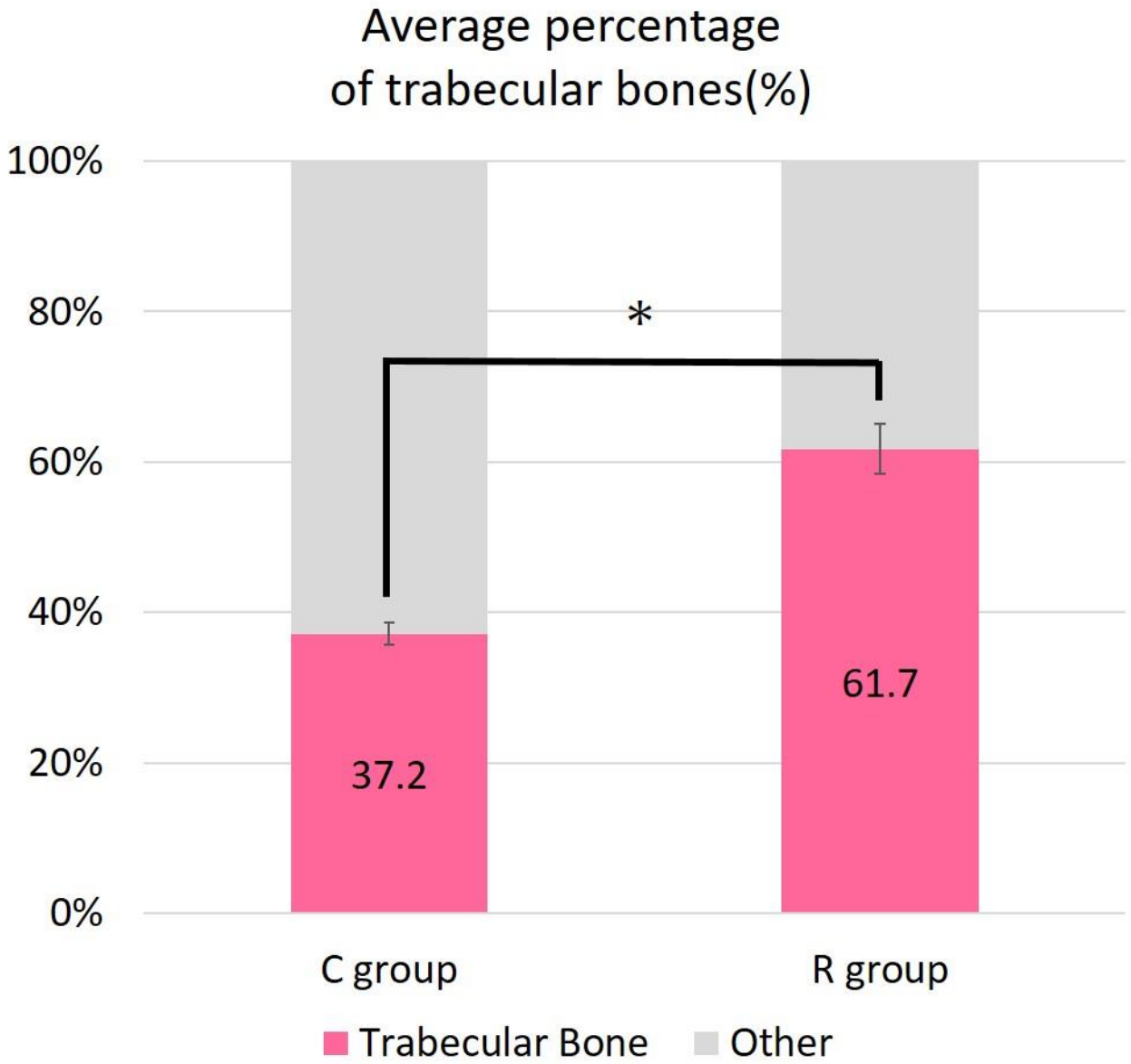
387



388

389

390 Figure 9. Percentage of bone trabeculae area in the pathological images at 20× magnification.



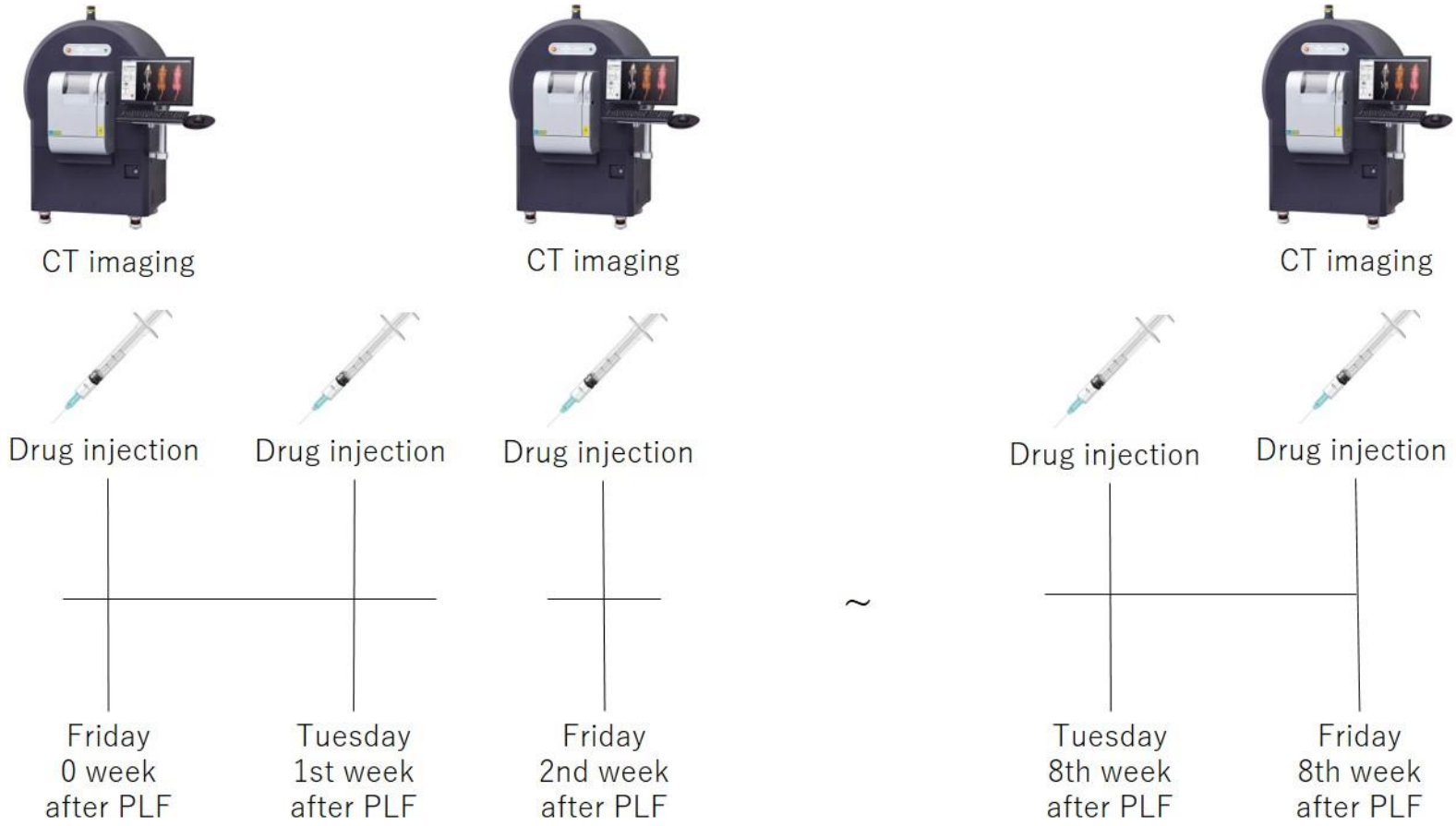
* : p < 0.05 by independent t test

391

392

393 **Table**

394 Table 1. Schedule of CT examination and drug administration



395

396